

On Energy-Efficient NOMA Designs for Heterogeneous Low-Latency Downlink Transmissions

Yanqing Xu, Chao Shen, Tsung-Hui Chang, Shih-Chun Lin, Yajun Zhao, and Gang Zhu

Abstract—This paper investigates energy-efficient resource allocation for the two-user downlink with strict latency constraints at users. To cope with strict latency constraints, the capacity formula of the finite blocklength codes (FBCs) is adopted, in contrast to the classical Shannon capacity formula. The FBC formula explicitly specifies the trade-off between blocklength and reliability. We first consider the case where the transmitter uses super-position coding based non-orthogonal multiple access (NOMA). However, due to heterogeneous latency constraints and channel conditions at users, the conventional successive interference cancellation may be infeasible. We thus propose to use different interference mitigation schemes according to heterogeneous user conditions and solve the corresponding NOMA design problems. Though the target energy function is non-convex and implicit, optimal user blocklength and power allocation can still be identified for the considered NOMA schemes and checking the problem feasibility is simple. It is observed that when the latency requirements are more heterogeneous, the NOMA scheme cannot achieve the best energy-efficiency of the downlink. In view of this, a hybrid transmission scheme which includes time division multiple access (TDMA) and NOMA as special cases is considered. Although the energy minimization is even challenging than the pure NOMA design problem, we propose a concave approximation of the FBC capacity formula which allows to obtain computationally efficient and high-quality solutions. Simulation results show that the hybrid scheme can benefit from both NOMA and TDMA.

Index Terms—Ultra-reliable and low-latency communications (URLLC), finite blocklength codes, energy efficiency, non-orthogonal multiple access

I. INTRODUCTION

The ultra-reliable and low-latency communication (URLLC) is one of the emerging application scenarios in 5G [2] [3], where the system promises to serve multiple autonomous machines with high reliability and low latency [4]–[6]. The traffic of such an URLLC system is drastically different from

that of the human-centric 4G LTE. More specifically, the communication is required to have no less than 99.999% reliability (that is, 10^{-5} packet error probability), no longer than 1ms latency, and small packet size (such as 32 bytes) [7]. Therefore, especially for multi-user channels, new system architectures and transmission schemes compared to the traditional human-centric communications are required to achieve the URLLC specifications. Moreover, energy-efficiency is a key performance indicator of 5G communications [8], and it is important to develop new energy-efficient transmissions for URLLC multi-user channels.

However, the existing energy-efficient transmission protocols only target at human-centric communications, and are based on the traditional Shannon capacity formula, such as [9] [10]. The Shannon capacity is accurate only when the codeword blocklength is infinitely long [11] [12], and thus not applicable to the URLLC system. Therefore, it motivates us to investigate the system design using the finite blocklength code (FBC). Recently, the maximal achievable rate of FBC in the Gaussian channel has been characterized in [13], and it is latter extended to the ergodic fading channel [14] and the outage-constrained slow fading channel [15]. The new capacity formula for FBC [13] explicitly characterizes the relationship between transmission rate, codeword blocklength and decoding reliability, and thus is particularly suitable for evaluating the performance of the URLLC system. Moreover, with only a 0.25dB loss, the information-theoretic capacity result in [13] can be practically approached via the polar code [16]. The capacity of FBC has been successfully applied to the study of various communication scenarios with strict latency constraints, as in [17]–[24]. In the context of energy-efficiency, [17] considered the energy-efficient packet scheduling problem in a point-to-point system and showed that using the classical Shannon capacity [11] can significantly underestimate the energy with the FBC.

As a promising enabling technique of 5G, the non-orthogonal multiple access (NOMA), which allows multiple users to transmit simultaneously over non-orthogonal channels, has been extensively studied [25] [26]. Indeed, for the downlink channel, the super-position coding based NOMA is shown to be capacity achieving when the blocklength is long [12]. Moreover, similar transmission scheme, known as the multiuser superposition transmission (MUST), has already been approved by the 3rd generation partnership project (3GPP) [27]. Compared to the orthogonal multiple access (OMA), NOMA can exploit the channel diversity more

Part of this work has been presented in IEEE Global Communication Conference (GlobeCom) Workshop on Ultra-Reliable and Low-Latency Communications, Dec., 2017, Singapore. [1].

Yanqing Xu, Chao Shen and Gang Zhu are with the State Key Laboratory of Rail Traffic Control and Safety, Beijing Jiaotong University, Beijing, China (email: {xuyanqing, chaoshen, gzhu}@bjtu.edu.cn).

Tsung-Hui Chang is with the School of Science and Engineering, The Chinese University of Hong Kong, Shenzhen, China, and also with the Shenzhen Research Institute of Big Data, Shenzhen, China (email: tsunghui.chang@ieee.org).

Shih-Chun Lin is with the Department of Department of Electronic and Computer Engineering, National Taiwan University of Science and Technology, Taipei, Taiwan (email: sclin@mail.ntust.edu.tw).

Yajun Zhao is with the Algorithm Department, Wireless Product R&D Institute, ZTE Corporation, Shenzhen, China (email: zhao.yajun1@zte.com.cn).

efficiently via smart interference management techniques such as the successive interference cancellation (SIC) [12] [25]. Recently, NOMA system designs with FBC attract lots of attentions [28]–[31]. In the downlink channels, [29] aims to minimize the common blocklengths of users while guaranteeing different reliability requirements; also under equal blocklengths, [30] considers the maximization of effective throughput. Finally, assuming all users experience equal channel conditions in the downlink, the FBC transmission by grouping users at the transmitter and decoding all user messages at each receiver is considered in [31]. All the former works [28]–[31] assume certain kinds of homogeneity such as the same blocklengths (latency constraints) or the same channel conditions. In practice, downlink users may ask for *heterogeneous* quality of service (QoS), and designing corresponding transmission protocols is crucial.

In this paper, we consider energy-efficient resource allocation for a two-user heterogeneous NOMA downlink with FBC. In particular, based on the superposition coding, we aim to solve the energy minimization problems subject to heterogeneous latency and reliability constraints at downlink users. Due to heterogeneous latency constraints (blocklength) and channel conditions, unlike downlinks with homogeneous constraints [29]–[31], SIC may not always be feasible since sometimes none of the receivers can decode messages of the other users. Thus for different combinations of channel conditions and latency constraints, we will consider different interference management techniques according to whether SIC is feasible or not. Solving our optimization problem is also challenging because the FBC capacity formula [13] does not admit a closed-form expression for our target energy function. Finally, unlike downlink with homogeneous latency constraints [12] [29] [30], we find out that in some channel conditions the NOMA scheme may cost larger energy than the OMA such as the time division multiple access (TDMA). Aim on this issue, we further present a hybrid transmission scheme which includes both NOMA and TDMA as special cases. Solving the corresponding energy minimization problems are even more challenging than those for the NOMA downlinks. The main contributions of this paper are summarized as follows.

- We optimally solve the energy minimization problems in NOMA downlinks under heterogeneous latency constraints and channel conditions, where SIC may be infeasible. Though the target energy is an *non-convex implicit function*, the *optimal* blocklengths and powers for users to minimize the total consumed energy can still be obtained. The key is identifying the monotonicity of the energy function with respect to user blocklengths with aids of the implicit function theorem [32]. Moreover, unlike the solver for TDMA [17], the *feasibility* of our solver for NOMA downlink can be simply checked.
- We propose a hybrid transmission scheme which consists of the NOMA and TDMA as special cases, and can be *strictly* better than both. However, the corresponding energy minimization is harder than that for only NOMA. We then find a *tight approximation* of the FBC capacity formula, with given blocklength and error probability,

to develop a suboptimal but computationally efficient solver. The efficiency results from the convexity of our approximation function and its inverse function. The resulted solver has much smaller complexity compared with the one based on naive linear search, and easy feasibility check inherited from NOMA.

Our simulation results with URLLC settings in 3GPP [7] [33] show that the superposition-coding based NOMA is more energy efficient than the TDMA when two latency constraints have small difference and are more homogeneous. Also the hybrid scheme can enjoy the benefits from the both. Finally, using traditional Shannon capacity formula would significantly under-estimate the consumed energy in the URLLC NOMA downlink.

Synopsis: Section II presents the energy minimization problems of NOMA schemes under heterogeneous user requirements. The hybrid transmission scheme is investigated in Section III with the convex approximation of FBC capacity presented in Section III-A. Simulation results with URLLC settings and Conclusions are presented in Section IV and V respectively.

II. SYSTEM MODEL AND ENERGY EFFICIENT NOMA SCHEMES

A. System model

We investigate an energy-efficient packet transmission problem in a downlink single-antenna system where a transmitter wants to send two private messages to two heterogeneous receivers respectively, as in Figure 1. According to the NOMA principle, the transmitter encodes the N_k message bits for receiver k into a codeword with block length m_k (symbols), $k = 1, 2$; and transmit the superposition of these two codewords to the receivers. The transmitted signal is then $\sqrt{p_1}x_1 + \sqrt{p_2}x_2$. Here x_1 and x_2 are the unit-power coded symbols of receiver 1 and receiver 2 respectively, and p_1 and p_2 are the transmission powers allocated to receiver 1 and receiver 2 respectively. The received signal for receiver k is given by

$$y_k = \tilde{h}_k(\sqrt{p_1}x_1 + \sqrt{p_2}x_2) + n_k, \quad k = 1, 2, \quad (1)$$

where $\tilde{h}_k \in \mathbb{C}$ is the channel coefficient of user k , and $n_k \sim \mathcal{CN}(0, \sigma_k^2)$ is the Gaussian noise at receiver k . Different from the traditional downlink schemes [12], *strict* latency constraints are imposed such that the codeword block length m_k must be smaller than D_k symbols (channel uses), $k = 1, 2$. To cope with the new latency constraints, we adopt the FBC capacity formula in [13] since the classical Shannon capacity formula is no longer appropriate.

Besides the encoder, the conventional SIC based decoders in [12] also need to be re-designed due to the latency constraints. Note that we consider *heterogeneous* receivers, that is, unlike [31] the channel gains can be unequal $|\tilde{h}_1| \neq |\tilde{h}_2|$ and unlike [29], [30] the latency constraints can also be different $D_1 \neq D_2$. Thus unlike [12], when $D_1 < D_2$ and $h_1 > h_2$, where $h_1 = |\tilde{h}_1|^2/\sigma_1^2$ and $h_2 = |\tilde{h}_2|^2/\sigma_2^2$ are the normalized channel gain at receiver 1 and receiver 2, respectively, receiver 1 *may not* be able to decode receiver 2's message and cancel

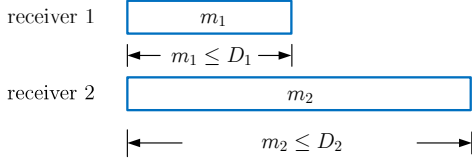


Fig. 1. Latency-constrained NOMA downlink, where the deadline D_2 of receiver 2 is longer than that of receiver 1.

the corresponding interference. Also, the signal y_2 received at receiver 2 may not be a degraded (always worse) version of y_1 . Thus one needs to design decoding strategies according to not only the channel gains h_k s but also the heterogeneous latency constraints D_k s. Without loss of generality, we assume $D_1 < D_2$ as in Figure 1 and consider two cases in this paper, that is, $h_1 \leq h_2$ and $h_1 > h_2$. The corresponding energy efficient transmission optimization problems are detailed in the next subsection

B. NOMA Transmission Under Different Channel Conditions

Case I ($h_1 \leq h_2$): Let us start from the case of $h_1 \leq h_2$. Since $D_1 < D_2$, receiver 2 can apply SIC if $m_1 \leq m_2$, whereas receiver 1 can only treat interference as noise. Specifically, for receiver 1, interference symbol x_2 is treated as Gaussian noise [13, equation(198)] in (1). Thus the achievable rate under FBC is given by [13] [17]

$$\frac{N_1}{m_1} = \log_2(1 + \gamma_1) - \sqrt{\frac{1}{m_1} \left(1 - \frac{1}{(\gamma_1 + 1)^2}\right) \frac{Q^{-1}(\epsilon_1)}{\ln 2}}, \quad (2)$$

where $\gamma_1 = \frac{p_1 h_1}{p_2 h_1 + 1}$ is the received signal-to-interference-plus-noise ratio (SINR) for receiver 1, ϵ_1 is the predefined block error probability for receiver 1, and $Q^{-1}(\cdot)$ is the inverse of the Gaussian Q-function¹. By the principle of SIC, receiver 2 would decode receiver 1's codeword with SINR $\frac{p_1 h_2}{p_2 h_2 + 1}$ in the first stage. Since $h_1 \leq h_2$, the SINR value $\frac{p_1 h_2}{p_2 h_2 + 1}$ is higher than γ_1 and therefore the SIC can achieve the corresponding block error probability ϵ_1 . By successfully subtracting x_1 from y_2 in (1) with probability $1 - \epsilon_1$, receiver 2 then decodes its private message, with probability $1 - \epsilon_2$, and achieves a rate satisfying

$$\frac{N_2}{m_2} = \log_2(1 + \gamma_2) - \sqrt{\frac{1}{m_2} \left(1 - \frac{1}{(\gamma_2 + 1)^2}\right) \frac{Q^{-1}(\epsilon_2)}{\ln 2}}, \quad (3)$$

where $\gamma_2 = p_2 h_2$ and ϵ_2 is the error probability conditioned on correct SIC. Note that the correct SIC needs that the decoding of interference, or user 1's codeword, be successful at receiver 2. The successful probability at stronger receiver 2 will be larger than the one at weaker receiver 1, i.e., $1 - \epsilon_1$. So the overall decoding error probability of receiver 2 is given by

$$\bar{\epsilon}_2 = (1 - \epsilon_1)\epsilon_2 + \epsilon_1 \quad (4a)$$

$$= \epsilon_1 + \epsilon_2 - \epsilon_1 \epsilon_2 \quad (4b)$$

¹ Compared with the AWGN capacity upper-bound in [13, equation (612)], achievable rate in (2) has loss within $\frac{\log(m_1) + \mathcal{O}(1)}{m_1}$

Based on the above models, the latency-constrained energy-efficient design problem when $h_1 < h_2$ is formulated as

$$\min_{\{m_k, p_k, \gamma_k\}_{k=1,2}} m_1 p_1 + m_2 p_2 \quad (5a)$$

$$\text{s. t. } F_k(m_k, \gamma_k) = 0, k = 1, 2, \quad (5b)$$

$$\hat{m} \leq m_k, k = 1, 2, \quad (5c)$$

$$m_1 \leq m_2, m_k \leq D_k, k = 1, 2, \quad (5d)$$

$$p_1 + p_2 \leq P_{\max}, 0 \leq p_k, k = 1, 2, \quad (5e)$$

$$\gamma_1 = \frac{p_1 h_1}{p_2 h_1 + 1}, \quad (5f)$$

$$\gamma_2 = p_2 h_2. \quad (5g)$$

where (5d) are the latency constraints, and (5b) are the FBC constraints with

$$F_k(m_k, \gamma_k) \triangleq \sqrt{\frac{1}{m_k} \left(1 - \frac{1}{(\gamma_k + 1)^2}\right) \frac{Q^{-1}(\epsilon_k)}{\ln 2}} - \log_2(1 + \gamma_k) + \frac{N_k}{m_k}. \quad (6)$$

Note that (5b) with $k = 1$ corresponds to (2), and (5b) with $k = 2$ corresponds to (3). Constraints (5c) represents the minimum blocklength constraint for (5b) holding true [13] [17] (typically $\hat{m} = 100$), while (5e) is the transmission power constraint.

Here we remark that solving problem (5) is challenging. In particular, the variables are coupled in the constraints in a non-convex and complex fashion. However, in upcoming Section II-C1, we will show how (5) can be globally solved.

Case II ($h_1 > h_2$): As aforementioned, unlike the case of $h_1 \leq h_2$, SIC may not be always feasible when $h_1 > h_2$ and $D_1 < D_2$. Thus we consider two scheduling policies as follows.

B.1 Full latency for receiver 2: In this case, we allow $m_1 \leq m_2$ since $D_1 < D_2$. Therefore, receiver 1 is not able to perform SIC, but instead treats x_2 as noise. Then the energy minimization problem is formulated as

$$\min_{\{m_k, p_k, \gamma_k\}} m_1 p_1 + m_2 p_2 \quad (7a)$$

$$\text{s. t. } (5b) - (5e), \quad (7b)$$

$$m_k \leq D_k, k = 1, 2, \quad (7b)$$

$$\gamma_1 = \frac{p_1 h_1}{p_2 h_1 + 1}, \quad (7c)$$

$$\gamma_2 = \frac{p_2 h_2}{p_1 h_2 + 1}. \quad (7d)$$

B.2 Short latency for receiver 2: In this case, we force

$$m_2 \leq m_1. \quad (8)$$

Note that $m_1 \leq D_1 < D_2$, thus the original latency constraint $m_2 \leq D_2$ is automatically satisfied. Under the setting of $m_2 \leq m_1$, SIC can be performed at receiver 1 to completely remove

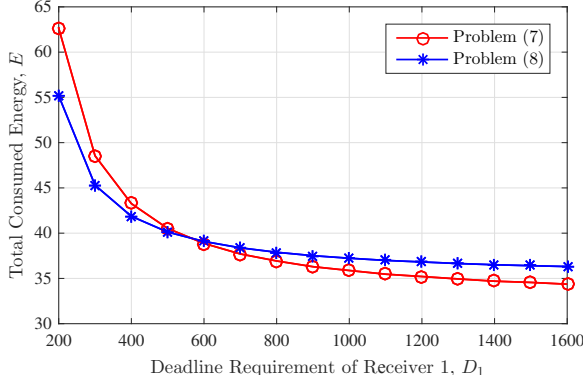


Fig. 2. Energy consumption comparison of problem (7) and (9) with $D_2 = 3800$, $h_1 = 100$, $h_2 = 10$, $\epsilon_1 = \epsilon_2 = 10^{-6}$, $N_1 = N_2 = 256$ bits and $P_{\max} = 40$ dBm.

the interference from receiver 2. Then the energy minimization problem is formulated as

$$\min_{\{m_k, p_k, \gamma_k\}} m_1 p_1 + m_2 p_2 \quad (9a)$$

$$\text{s. t.} \quad (5b) - (5e),$$

$$m_1 \leq D_1, \quad m_2 \leq m_1, \quad (9b)$$

$$\gamma_1 = p_1 h_1, \quad (9c)$$

$$\gamma_2 = \frac{p_2 h_2}{p_1 h_2 + 1}. \quad (9d)$$

The solutions of aforementioned two problems are given in Section II-C2. Here we point out that problem (9) can yield a smaller energy than (7) when the two deadlines D_2 and D_1 are close, thanks to the performance gain brought by SIC. However, when D_2 is significantly larger than D_1 , formulation (7) can become more energy efficient by benefiting from long code transmission as shown in Fig. 2.

C. Optimal Solutions of NOMA Transmission Problems

In this subsection, we present the solutions to the NOMA problems in (5), (7), and (9).

1) *Optimal Solutions for Problem (5)*: By (5b) and by applying the implicit function theorem [32], there exist continuously differentiable implicit functions $\Gamma_k(\cdot)$ such that

$$\Gamma_k(m_k) = \gamma_k, k = 1, 2. \quad (10)$$

Note that $\Gamma_k(m_k)$ can be treated as the SINR function with respect to blocklength m_k . Thus from (5g), we have

$$p_1 = \frac{\gamma_1 \gamma_2}{h_2} + \frac{\gamma_1}{h_1} = \frac{\Gamma_1(m_1) \Gamma_2(m_2)}{h_2} + \frac{\Gamma_1(m_1)}{h_1}, \quad (11a)$$

$$p_2 = \frac{\gamma_2}{h_2} = \frac{\Gamma_2(m_2)}{h_2}. \quad (11b)$$

Then by (10), we can rewrite the target energy of (5a) as a function of block length m_k s as

$$\frac{m_1 \Gamma_1(m_1) (\Gamma_2(m_2) h_1 / h_2 + 1)}{h_1} + \frac{m_2 \Gamma_2(m_2)}{h_2}. \quad (12)$$

Now we have the following Lemma.

Lemma 1 Function $E_k(m_k) \triangleq m_k \Gamma_k(m_k)$ is strictly decreasing with blocklength $m_k \in [\hat{m}, \infty)$ provided that the error probability ϵ_k and packet size N_k satisfy

$$\frac{Q^{-1}(\epsilon_k)}{\sqrt{N_k}} \leq \frac{2\sqrt{\ln 2}}{4 - \sqrt{2}} = 0.64394 \dots \quad (13)$$

Proof: The proof is relegated to Appendix A. ■

It is worthwhile to note that comparing to [17, Proposition 1], condition (13) is less restrictive as it allows the monotonicity holds under much milder conditions (e.g., $\epsilon_k \geq 10^{-10}$ and $N_k \geq 100$). Indeed, (13) is satisfied in the URLLC system, where the typically required codeword error probability is 10^{-6} and the packet size is around 256 bits (32 bytes) [7]. Based on the monotonicity presented in Lemma 1, we can obtain the global optimal solution to problem (5) as follows.

Theorem 1 Suppose that (13) is met and that problem (5) is feasible. The optimal solution to problem (5) is given by

$$\begin{cases} m_k^* = D_k, & \text{for } k = 1, 2, \\ \gamma_k^* = \Gamma_k(D_k), & \text{for } k = 1, 2, \\ p_1^* = \frac{\gamma_1^* \gamma_2^*}{h_2} + \frac{\gamma_1^*}{h_1} = \frac{\Gamma_1(D_1) \Gamma_2(D_2)}{h_2} + \frac{\Gamma_1(D_1)}{h_1}, \\ p_2^* = \frac{\gamma_2^*}{h_2} = \frac{\Gamma_2(D_2)}{h_2}, \end{cases} \quad (14)$$

where the implicit function $\Gamma_k(\cdot)$ satisfy (10) and the optimal SINR $\gamma_k^* = \Gamma_k(D_k)$ can be obtained through Algorithm 1.

Proof: We first claim that (5d) must hold with equality at the optimum, i.e., the optimal blocklengths must be $m_k^* = D_k$ for all $k = 1, 2$. Suppose that this is not true, i.e., $m_k^* < D_k$ for $k = 1$ or $k = 2$. Then one can further increase m_k^* . According to [17, Proposition 1], $\Gamma_k(m_k)$ is monotonically decreasing with $m_k > 0$. Since

$$p_1 + p_2 = \frac{\Gamma_1(m_1) \Gamma_2(m_2)}{h_2} + \frac{\Gamma_1(m_1)}{h_1} + \frac{\Gamma_2(m_2)}{h_2}, \quad (15)$$

$p_1^* + p_2^*$ can be reduced without violating (5e) when m_k^* increases. Besides, by Lemma 1, we also know that $m_k \Gamma_k(m_k)$ is decreasing with m_k . Thus the energy function in (12) can be reduced when m_k^* increases. These two facts contradict with the optimality of m_k^* . So we must have $m_k^* = D_k$ for all $k = 1, 2$. Correspondingly, $\gamma_k^* = \Gamma_k(m_k^*)$ from (10) and p_k^* can be obtained from (11) accordingly, which lead to the optimal solution in (14).

Finally, note that $\gamma_k = \Gamma_k(m_k)$ from (10) is strictly decreasing with m_k [17, Proposition 1], and thus the optimal and unique SINR $\gamma_k^* = \Gamma_k(D_k)$ can be efficiently computed by the bisection search in Algorithm 1 [34]. Interestingly, by (5b), the inverse of implicit function $\Gamma_k^{-1}(\gamma_k)$ can be expressed in closed-form as (16). ■

Remark 1 Note that for given block error rate and latency requirements, problem (5) may not be feasible due to the limited P_{\max} and the deep channel fadings. However, thanks to the obtained closed-form solution of problem (5) in (14), its feasibility can be easily checked. In particular, from the proof of Theorem 1, if

$$\frac{\Gamma_1(D_1) \Gamma_2(D_2)}{h_2} + \frac{\Gamma_1(D_1)}{h_1} + \frac{\Gamma_2(D_2)}{h_2} \leq P_{\max}, \quad (17)$$

Algorithm 1 Algorithm to find optimal SINR for problem (5)

```

1: Given the initial values  $\Gamma_{\ell k} = 0, \Gamma_{uk} = P_{\max} h_k + \delta$  with  $\delta > 0$ ,
   and the tolerance  $\epsilon_0$ .
2: while  $\Gamma_{uk} - \Gamma_{\ell k} > \epsilon_0$  do
3:    $\bar{\gamma}_k = \frac{1}{2}(\Gamma_{uk} + \Gamma_{\ell k})$ .
4:   Compute  $\bar{m}_k = \Gamma_k^{-1}(\bar{\gamma}_k)$  as
      
$$\left[ \frac{1}{2 \log_2(1 + \bar{\gamma}_k)} \left( \frac{Q^{-1}(\epsilon_k)}{\ln 2} \sqrt{1 - \frac{1}{(\bar{\gamma}_k + 1)^2}} \right. \right. \\ \left. \left. + \sqrt{\left( 1 - \frac{1}{(\bar{\gamma}_k + 1)^2} \right) \left( \frac{Q^{-1}(\epsilon_k)}{\ln 2} \right)^2 + 4 N_k \log_2(1 + \bar{\gamma}_k)} \right) \right]^2 \quad (16)$$

5:   if  $\bar{m}_k < m_k^*$  then
6:     Update  $\Gamma_{uk} = \bar{\gamma}_k$ .
7:   else
8:     Update  $\Gamma_{\ell k} = \bar{\gamma}_k$ .
9:   end if
10: end while
Ensure:  $\gamma_k^* = \Gamma_k(m_k^*)$ 

```

the problem (5) is feasible under P_{\max} and for channel realizations (h_1, h_2) . Otherwise, problem (5) is infeasible.

Remark 2 It is important to point out that the overall communication reliability of receiver k is the product of the receiver decoding probability and the feasibility of problem (5). For instance, assume the infeasible probability of the problem (5) is ϵ_{ifp} , the overall reliability for receiver 2 should be $(1 - \bar{\epsilon}_2)(1 - \epsilon_{\text{ifp}}) \approx 1 - \bar{\epsilon}_2 - \epsilon_{\text{ifp}}$, where $\bar{\epsilon}_2$ is given in (4). Note that for given block error rate and latency requirements, the feasibility of the optimization problems is determined by P_{\max} and the random channel realizations. Thus, for given distribution of the channel gain, the block error rate and P_{\max} should be jointly selected to guarantee the communication reliability of the receivers, which will be studied in the simulation section.

2) *Optimal Solutions for Problem (7) and (9):* Similar to problem (5), the optimal solutions of problem (7) and (9) can be obtained by using the monotonicity in Lemma 1, which are summarized in the following corollaries.

Corollary 1 If condition (13) is met, the optimal solution of problem (7) is given by

$$\begin{cases} m_k^* = D_k, & \text{for } k = 1, 2, \\ \gamma_k^* = \Gamma_k(D_k), & \text{for } k = 1, 2, \\ p_1^* = \frac{\gamma_1^* h_2 + \gamma_1^* \gamma_2^* h_1}{h_1 h_2 (1 - \gamma_1^* \gamma_2^*)}, \\ p_2^* = \frac{\gamma_2^* h_1 + \gamma_1^* \gamma_2^* h_2}{h_1 h_2 (1 - \gamma_1^* \gamma_2^*)}, \end{cases} \quad (18)$$

whenever it is feasible, where the optimal SINR γ_k^* ($k = 1, 2$) can be obtained through Algorithm 1.

Corollary 2 If condition (13) is met, the optimal solution of problem (9) is given by

$$\begin{cases} m_k^* = D_1, & \text{for } k = 1, 2, \\ \gamma_k^* = \Gamma_k(D_1), & \text{for } k = 1, 2, \\ p_1^* = \frac{\gamma_1^*}{h_1}, \\ p_2^* = \frac{\gamma_1^* \gamma_2^*}{h_1} + \frac{\gamma_2^*}{h_2}, \end{cases} \quad (19)$$

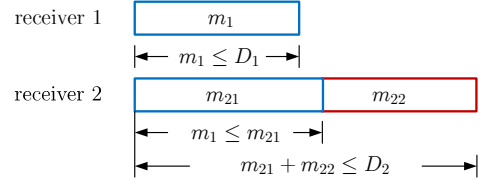


Fig. 3. Hybrid transmission scheme where the packet of receiver 2 is split into two parts which are scheduled with m_{21} and m_{22} symbols respectively. Here $h_1 \leq h_2$ and receiver 2 performs SIC.

whenever it is feasible, where the optimal SINR γ_k^* ($k = 1, 2$) can be obtained through Algorithm 1.

Proof: The proofs of Corollary 1 and 2 are similar to that of Theorem 1. Thus we omit it here. ■

It is important to point out that, due to the heterogeneous latency requirements ($D_1 < D_2$) of the receivers, the proposed NOMA scheme is conservative and *cannot* achieve the same energy efficiency of traditional NOMA schemes that assume perfect SIC [26]. Specifically, when $h_1 < h_2$, we have assumed that receiver 2 performs SIC given that the interfering signal from receiver 1 has the same blocklength as the signal of receiver 2. However, in fact, there is no interference during the last $D_2 - D_1$ symbols; on the other hand, when receiver 1 performs SIC for $h_1 \geq h_2$, it needs $m_2 = m_1 = D_1 < D_2$. Thus the blocklength of receiver 2 is limited, which would incur more energy consumption according to Lemma 1. With this consideration, we investigate a novel hybrid transmission scheme in the ensuing sections.

III. PROPOSED HYBRID NOMA TRANSMISSION SCHEMES

In this section, we introduce data splitting with time domain power allocation to NOMA and propose a hybrid scheme that incorporate the NOMA in the previous section and TDMA as special cases. In particular, the data packet for user 2 is split into two parts, where the first part has N_{21} bits and the second has N_{22} bits and $N_{21} + N_{22} = N_2$. The N_{21} bits are encoded into m_{21} symbols, and combined with the encoded symbols for user 1 using the non-orthogonal super-position coding; whereas the rest N_{22} bits are encoded into m_{22} symbols and scheduled in the non-overlapping time slots. Note that when $N_{21} = 0$, the hybrid scheme degrades into the TDMA studied in [17]; while when $N_{22} = 0$, the hybrid scheme degrades into the NOMA in Section II. As in Section II-B, according to the different channel conditions at receivers, we study the problem by considering the following cases.

Case I ($h_1 \leq h_2$ with SIC at receiver 2) : In this case, the transmission scheme is sketched in Fig. 3 and receiver 2 performs SIC. The transmitter first transmits the N_1 bits of receiver 1 and N_{21} bits of receiver 2 by using the NOMA scheme. The transmit signal is $\sqrt{p_1}x_1 + \sqrt{p_{21}}x_{21}$, where x_{21} and p_{21} are the unit-power coded symbols and corresponding allocated power for user 2, respectively. Also we have $p_1 + p_{21} \leq P_{\max}$.

For user 1, the N_1 bits are encoded with a FBC with length m_1 and the achievable rate is same as (2) with SINR $\gamma_1 = \frac{p_1 h_1}{p_2 h_1 + 1}$. For receiver 2, it can cancel the interference from user 1 using the received from the first m_{21} received symbols since $\frac{p_1 h_2}{p_2 h_2 + 1} > \gamma_1$. After that, receiver 2 decodes its own information with SINR $\gamma_{21} = p_{21} h_2$, and from the corresponding achievable rate $\frac{N_{21}}{m_{21}}$ satisfies

$$\frac{N_{21}}{m_{21}} = \log_2(1 + \gamma_{21}) - \sqrt{\frac{1}{m_{21}} \left(1 - \frac{1}{(\gamma_{21} + 1)^2}\right)} \frac{Q^{-1}(\epsilon_{21})}{\ln 2}. \quad (20)$$

Remind that receiver 2 needs to receive all information symbols of receiver 1 to perform SIC, thus we require that

$$m_{21} \geq m_1. \quad (21)$$

Once the transmission of the first m_{21} symbols is complete, the transmitter starts to deliver the rest N_{22} bits solely for user 2 using m_{22} symbols and power p_{22} . The achievable rate $\frac{N_{22}}{m_{22}}$ satisfies

$$\frac{N_{22}}{m_{22}} = \log_2(1 + \gamma_{22}) - \sqrt{\frac{1}{m_{22}} \left(1 - \frac{1}{(\gamma_{22} + 1)^2}\right)} \frac{Q^{-1}(\epsilon_{22})}{\ln 2}, \quad (22)$$

where $\gamma_{22} = p_{22} h_2$. Notice that the SIC at receiver 2 is successful only when the interference (from user 1's message) is perfectly subtracted as well as the N_{21} and N_{22} bits are both successfully decoded. Also for the decoding of user 1's codeword, the successful probability at stronger receiver 2 will be larger than the one at weaker receiver 1, i.e., $1 - \epsilon_1$. Then the overall block error rate for receiver 2 is upper-bounded by

$$\epsilon_2 = 1 - (1 - \epsilon_1)(1 - \epsilon_{21})(1 - \epsilon_{22}). \quad (23)$$

With slightly abuse of notations, the implicit SINR function in (10) is denoted as $\gamma_k \triangleq \Gamma_k(N_k, m_k)$. Therefore, the energy minimization problem can be formulated as follows

$$\min_{\substack{N_{21}, N_{22}, \\ m_1, m_{21}, m_{22}, \\ p_1, p_{21}, p_{22}}} m_1 p_1 + m_{21} p_{21} + m_{22} p_{22} \quad (24a)$$

$$\text{s. t. } \gamma_1 = \frac{p_1 h_1}{p_2 h_1 + 1} = \Gamma_1(N_1, m_1), \quad (24b)$$

$$\gamma_{21} = p_{21} h_2 = \Gamma_{21}(N_{21}, m_{21}), \quad (24c)$$

$$\gamma_{22} = p_{22} h_2 = \Gamma_{22}(N_{22}, m_{22}), \quad (24d)$$

$$m_1 \leq \min\{D_1, m_{21}\}, \quad (24e)$$

$$m_{21} + \text{sgn}(N_{22}) m_{22} \leq D_2, \quad (24f)$$

$$m_1, m_{21}, m_{22} \geq \hat{m}, \quad (24g)$$

$$p_1 + p_{21} \leq P_{\max}, p_{22} \leq P_{\max}, \quad (24h)$$

$$p_1, p_{21}, p_{22} \geq 0, \quad (24i)$$

$$N_{21} + N_{22} = N_2, 0 \leq N_{21} \leq N_2. \quad (24j)$$

where $\text{sgn}(\cdot)$ denotes the sign function, and satisfies $\text{sgn}(N_{22}) = 0$ with $N_{22} = 0$, $\text{sgn}(N_{22}) = 1$ with $N_{22} \geq 1$. Note that when $N_{21} = 0$ problem (24) degrades to energy minimization with TDMA; and when $N_{22} = 0$, problem (24) degrades into (5) with pure NOMA. Since (5) has been already optimally solved in Section II-C, we only need to focus on the

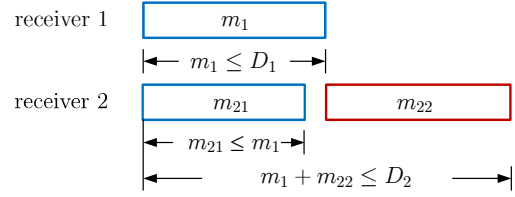


Fig. 4. Hybrid transmission scheme when $h_2 \leq h_1$ and receiver 1 performs SIC.

cases of $0 \leq N_{21} \leq N_2 - 1$ (thus $N_{22} \geq 1$) in problem (24) in the upcoming solver.

Case 2 ($h_2 < h_1$ with SIC at receiver 1): In this case, receiver 1 performs SIC to cancel the interference from user 2 and the transmission scheme is depicted in Fig. 4. To satisfy the requirement of SIC at receiver 1, the latency constraints are given by

$$m_{21} \leq m_1 \leq D_1, \quad (25a)$$

$$m_1 + m_{22} \leq D_2, \quad (25b)$$

$$m_1, m_{21}, m_{22} \geq \hat{m}. \quad (25c)$$

The energy minimization problem can be formulated as

$$\min_{\substack{N_{21}, N_{22}, \\ m_1, m_{21}, m_{22}, \\ p_1, p_{21}, p_{22}}} m_1 p_1 + p_{21} m_{21} + p_{22} m_{22} \quad (26a)$$

$$\text{s. t. } (24d), (24h), (24i), (24j), (25), \quad (26b)$$

$$\gamma_1 = p_1 h_1 = \Gamma_1(N_1, m_1), \quad (26c)$$

$$\gamma_{21} = \frac{p_{21} h_2}{p_1 h_2 + 1} = \Gamma_{21}(N_{21}, m_{21}) \quad (26d)$$

Here we should point out that problems (24) and (26) are more challenging to solve compared to problems (5), (7) and (9) in Section II due to the following reasons. First, the blocklengths m_{21} and m_{22} of user 2 in the two transmission stages are coupled in the constraints, consequently, the monotonicity of the energy function *cannot* be used to attain the solution directly as in Section II. Second, now the integer packet sizes N_{21} and N_{22} of user 2 are the additional optimization variables, which also complicates the constraints (24c) and (24d). To solve these problems efficiently, a concave approximation of the FBC capacity formula is provided next.

A. Convex Approximation of the FBC Capacity

We start from the convexity analysis of the FBC capacity as in upcoming Proposition 1 and then propose a concave approximation of the FBC capacity in (33), with given blocklength and error probability. The inverse of proposed approximation function (33) is also convex. For the simplicity of notation, we remove the subindex of all variables and let x denote the SINR. The FBC capacity formula then becomes

$$\frac{N}{m} = \ln(1 + x) - \sqrt{\frac{1}{m} \left(1 - \frac{1}{(1 + x)^2}\right)} \frac{Q^{-1}(\epsilon)}{\ln(2)}. \quad (27)$$

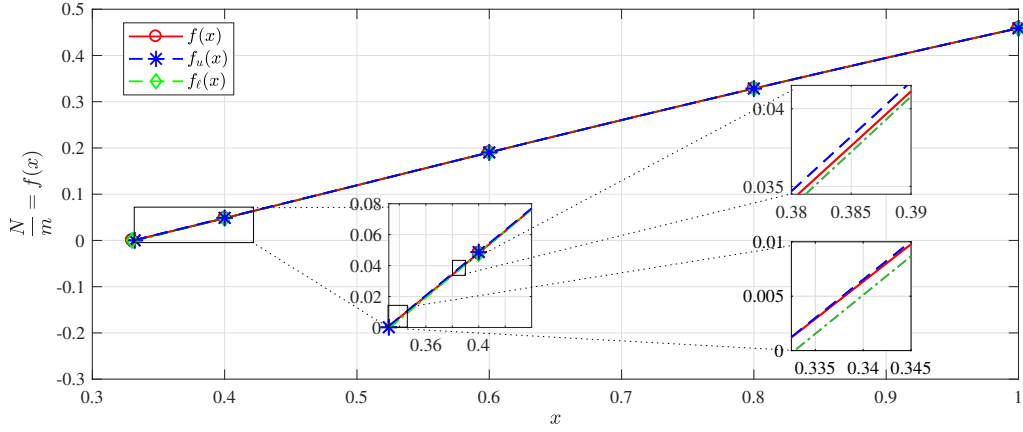
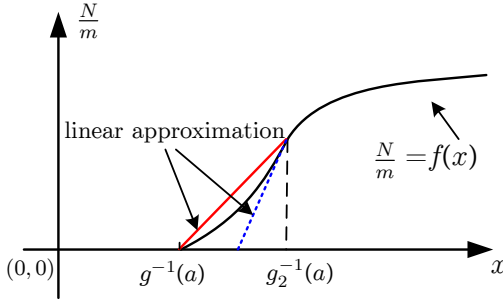
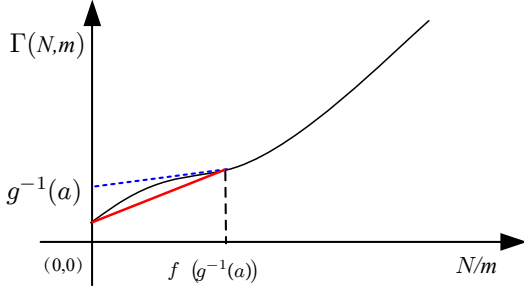


Fig. 5. Comparison of FBC capacity formula and its approximations; here $m = 300$ and $\epsilon = 10^{-7}$, and correspondingly $a = 0.4431$.



(a) FBC capacity function $f(x)$ for the case $a \leq \beta$ in Proposition 1.



(b) The inverse function of $f(x)$, or the SINR function $\Gamma(N, m)$ with fixed m , for the cases of $a \leq \beta$.

Fig. 6. Illustration of the convexity of FBC capacity function $f(x)$ and its inverse function.

With given blocklength m and error probability ϵ , by letting $a = \frac{Q^{-1}(\epsilon)}{\sqrt{m \ln 2}}$, we define $f(x)$ as

$$f(x) \triangleq \ln(x+1) - a \frac{\sqrt{x(x+2)}}{x+1} \quad (28)$$

Also, given m , we define SINR function with respect to packet size as $\Gamma(N, m) = f^{-1}(\frac{N}{m})$. Then we have the following proposition, with the proof relegated to Appendix B, as

Proposition 1 Let constant $\beta \triangleq g(x_0) = g_2(x_0)$, where $x_0 = 0.6904$ is the positive solution of equation $g_2(x) = g(x)$ with

$$g_2(x) \triangleq \frac{(x+1)(x(x+2))^{\frac{3}{2}}}{3x^2 + 6x + 1} \quad (29a)$$

$$g(x) \triangleq \frac{(x+1) \ln(x+1)}{\sqrt{x(x+2)}}. \quad (29b)$$

For a given a , the convexity of $f(x)$ in (28) is given by

$$\begin{cases} \text{if } a > \beta, f(x) \text{ is concave and increasing for } x > g^{-1}(a), \\ \text{if } a \leq \beta, \\ \begin{cases} f(x) \text{ is concave and increasing for } x > g_2^{-1}(a), \\ f(x) \text{ is convex and increasing for } g^{-1}(a) \leq x \leq g_2^{-1}(a). \end{cases} \end{cases} \quad (30)$$

Note that only positive $f(x)$ is meaningful by definition, so x must be larger than $g^{-1}(a)$ from (28). Besides, whenever $f(x)$ is concave in x , $\Gamma(N, m)$ is convex in N .

Proposition 1 shows that $f(x)$ ($\Gamma(N, m)$) is not always concave (convex). To overcome this problem, as shown in Fig. 6(a), we consider approximating $f(x)$ in the interval $g^{-1}(a) \leq x < g_2^{-1}(a)$ by taking a linear upper bound and lower bound. Specifically, since $f(x)$ is convex in the interval $g^{-1}(a) \leq x < g_2^{-1}(a)$ for $a \leq \beta$, the linear function

$$f_u(x) = \frac{f(g_2^{-1}(a))}{g_2^{-1}(a) - g^{-1}(a)} (x - g^{-1}(a)); \quad (31)$$

is an upper bound of $f(x)$; the first-order Tylor expansion of $f(x)$ at $x = g_2^{-1}(a)$, i.e.,

$$f_l(x) = f'(g_2^{-1}(a)) (x - g_2^{-1}(a)) + f(g_2^{-1}(a)). \quad (32)$$

is a lower bound of $f(x)$.

In Fig. 5, we show the tightness of these two approximations, and the linear approximation is applied in the interval where $0.3307 = g^{-1}(a) \leq x \leq g_2^{-1}(a) = 0.4921$.

Although both of the linear approximations are quite tight from Fig. 5, we will use the lower-bound approximation (32). First, the lower-bound approximation can be treated as an achievable rate. Second, by using the lower-bound approximation, the approximated FBC capacity formula $f(x)$ is a concave function. Then the corresponding SINR function

$\Gamma_k(\cdot)$ in Problems (24) and (26), is increasing and convex in the (normalized) number of data bits N/m [35, Proposition 2]. An example is shown in Fig 6(b). In the meanwhile, with the upper-bound approximation, the approximated FBC formula is only quasi-concave, and thus the convexity of SINR functions cannot be guaranteed. Finally, by using (32), the approximation of the FBC capacity with given blocklength m and error probability (30) reads

$$\frac{N}{m} = f_M(x) \triangleq \begin{cases} \ln(x+1) - a \frac{\sqrt{x(x+2)}}{x+1}, & \text{if } \begin{cases} a > \beta & \& x \geq g^{-1}(a) \\ a \leq \beta & \& x \geq g_2^{-1}(a) \end{cases} \\ (32), & \text{if } a \leq \beta \& g^{-1}(a) \leq x < g_2^{-1}(a). \end{cases} \quad (33)$$

where x is the SINR while a and β are given in Proposition 1.

B. Solving Problems (24) and (26) with Approximation (33)

Now we turn to solve the mixed-integer problems (24) and (26). Since (24) and (26) have similar structures we first focus on problem (24). We first provide a solver based on exhaustive linear search as a benchmark, and then present a more efficient one based on Lemma 1 and approximation (33).

Benchmark : solver using exhaustive linear search : Note that the SINR constraints and transmit power constraints in (24h) and (24i) actually restrict the packet size and blocklengths to a subset that

$$\mathcal{H} \triangleq \left\{ N_{21}, m_1, m_{21}, m_{22} \mid \begin{aligned} p_1 &= \frac{\Gamma_1(N_1, m_1) \Gamma_{21}(N_{21}, m_{21})}{h_2} + \frac{\Gamma_1(N_1, m_1)}{h_1}, \\ p_{21} &= \frac{\Gamma_{21}(N_{21}, m_{21})}{h_2}, p_{22} = \frac{\Gamma_{22}(N_2 - N_{21}, m_{22})}{h_2} \\ &\text{and (24h) and (24i) are satisfied} \end{aligned} \right\}. \quad (34)$$

Thus problem (24) can be rewritten as

$$\min_{\substack{N_{21}, m_1, \\ m_{21}, m_{22}}} \frac{m_1 \Gamma_1(N_1, m_1)}{h_1} + \frac{m_1 \Gamma_1(N_1, m_1) \Gamma_{21}(N_{21}, m_{21})}{h_2} + \frac{m_{21} \Gamma_{21}(N_{21}, m_{21})}{h_2} + \frac{m_{22} \Gamma_{22}(N_2 - N_{21}, m_{22})}{h_2} \quad (35a)$$

$$\text{s. t. } m_1 \leq \min\{m_{21}, D_1\}, \quad (35b)$$

$$m_{21} + m_{22} = D_2, \quad (35c)$$

$$m_1, m_{21}, m_{22} \geq \hat{m}, \quad (35d)$$

$$N_{21} + N_{22} = N_2, \quad (35e)$$

$$0 \leq N_{21} \leq N_2 - 1, \quad (35f)$$

$$(N_{21}, m_1, m_{21}, m_{22}) \in \mathcal{H}, \quad (35g)$$

where the “=” in (35c) is attained from Lemma 1. It can be readily verified that, by ignoring constraint (35g), problem (35) is fully determined by variables N_{21} , m_1 and m_{21} . Thus it can be solved to its global optimal solutions by using a 3-D exhaustive search method as stated in Algorithm 2, in which steps 8 – 12 is to guarantee the obtained solution is feasible to problem (35).

Algorithm 2 Benchmark : 3-D linear search for energy minimization problem (35)

```

1: for  $N_{21} = 1 : N_2 - 1$ 
2:    $N_{22} = N_2 - N_{21}$ ;
3:   for  $m_1 = \hat{m} : \min\{D_1, D_2 - \hat{m}\}$ 
4:     for  $m_{21} = m_1 : D_2 - \hat{m}$ 
5:        $m_{22} = D_2 - m_{21}$ ;
6:       Obtain  $\Gamma_1$ ,  $\Gamma_{21}$  and  $\Gamma_{22}$  through bisection search method.
7:       Calculate  $p_1$ ,  $p_{21}$ ,  $p_{22}$  based on (24b), (24c) and (24d).
8:       if  $(N_{21}, m_1, m_{21}, m_{22}) \in \mathcal{H}$ .
9:         Calculate  $E_n$  based on (35a).
10:      else.
11:         $E_n = +\text{Inf}$ .
12:      end if.
13:    end for
14:  end for
15: end for
16: Output:  $E_n^{\text{opt}} = \min\{E_n\}$ ;

```

The complexity of Algorithm 2 is determined by linear searching of N_{21} with complexity order $\mathcal{O}(N_2)$, those of m_1 and m_{21} with complexity order $\mathcal{O}\left(\frac{1}{2}(2D_2 - 3\hat{m} + 2 - \min\{D_1, D_2 - \hat{m}\})(\min\{D_1, D_2 - \hat{m}\} + 2 - \hat{m})\right)$. Besides, in each iteration, it contains 3 times bisection search to find the optimal SINRs with complexity order of $\mathcal{O}\left(3 \log\left(\frac{\max_k\{h_k P_{\max}\}}{\epsilon_0}\right)\right)$ where $\epsilon_0 > 0$ is the desired accuracy. Summarily, the total complexity order is given by $\mathcal{O}\left(\frac{3N_2}{2}(2D_2 - 3\hat{m} + 2 - \min\{D_1, D_2 - \hat{m}\})(\min\{D_1, D_2 - \hat{m}\} + 2 - \hat{m}) \log\left(\frac{\max_k\{h_k P_{\max}\}}{\epsilon_0}\right)\right)$. Considering the high computational complexity of the 3-D linear search, we seek a more efficient way to solve problem (35).

Solver based on Convex Approximation : Now we present the solver which is more efficient than the previous one using three-dimensional linear search. First by properly utilizing the latency constraints, problem (35) can be decoupled into two subproblems each can be solved by two-dimensional linear search. Then with aids of the convex approximation of FBC capacity, the search range can be significantly reduced. More specifically, based on (35b) and Lemma 1, problem (35) can be decoupled as cases (a) and (b) in the following

a) $m_{21} < D_1$: In this case, we have $m_1 = m_{21}$ from Lemma 1 and thus the objective function of problem (35) becomes

$$\frac{m_{21} \Gamma_1(N_1, m_{21})}{h_1} + \frac{m_{21} \Gamma_1(N_1, m_{21}) \Gamma_{21}(N_{21}, m_{21})}{h_2} + \frac{m_{21} \Gamma_{21}(N_{21}, m_{21})}{h_2} + \frac{(D_2 - m_{21}) \Gamma_{22}(N_2 - N_{21}, D_2 - m_{21})}{h_2}; \quad (36)$$

and by ignoring constraint (35g), problem (35) becomes

$$\min_{N_{21}, m_{21}} \frac{m_{21} \Gamma_1(N_1, m_{21})}{h_1} + \frac{(m_{21} \Gamma_1(N_1, m_{21}) + m_{21}) \Gamma_{21}(N_{21}, m_{21})}{h_2} + \frac{(D_2 - m_{21}) \Gamma_{22}(N_2 - N_{21}, D_2 - m_{21})}{h_2} \quad (37a)$$

$$\text{s. t. } \hat{m} \leq D_2 - m_{21}, \quad (37b)$$

$$\hat{m} \leq m_{21} \leq D_1, \quad (37c)$$

$$0 \leq N_{21} \leq N_2 - 1. \quad (37d)$$

b) $m_{21} \geq D_1$: In this case, we have $m_1 = D_1$ from Lemma 1 and the objective function of problem (35) becomes

$$\frac{D_1 \Gamma_1(N_1, D_1)}{h_1} + \frac{D_1 \Gamma_1(N_1, D_1) \Gamma_{21}(N_{21}, m_{21})}{h_2} + \frac{m_{21} \Gamma_{21}(N_{21}, m_{21})}{h_2} + \frac{(D_2 - m_{21}) \Gamma_{22}(N_2 - N_{21}, D_2 - m_{21})}{h_2} \quad (38a)$$

$$= \frac{(m_{21} + D_1 \Gamma_1(N_1, D_1)) \Gamma_{21}(N_{21}, m_{21})}{h_2} + \frac{(D_2 - m_{21}) \Gamma_{22}(N_2 - N_{21}, D_2 - m_{21})}{h_2} + \frac{D_1 \Gamma_1(N_1, D_1)}{h_1}. \quad (38b)$$

Therefore by ignoring constraint (35g), problem (35) is equivalent to

$$\min_{N_{21}, m_{21}} \left(m_{21} + D_1 \Gamma_1(N_1, D_1) \right) \Gamma_{21}(N_{21}, m_{21}) + (D_2 - m_{21}) \Gamma_{22}(N_2 - N_{21}, D_2 - m_{21}) \quad (39a)$$

$$\text{s. t. } \hat{m} \leq D_2 - m_{21}, \quad (39b)$$

$$D_1 \leq m_{21}, \quad (39c)$$

$$0 \leq N_{21} \leq N_2 - 1. \quad (39d)$$

Notice that problem (37) and (39) are determined by variables m_{21} and N_{21} , indicating that problem (35) can be solved by 2-D linear search of m_{21} and N_{21} . Remind that we decouple problem (35) based on the value of m_{21} , thus we do linear search of m_{21} first and then find the optimal N_{21} . Specifically, for given m_{21} , problem (37) degrades into

$$\min_{N_{21}} (m_{21} \Gamma_1(N_1, m_{21}) + m_{21}) \Gamma_{21}(N_{21}, m_{21}) + (D_2 - m_{21}) \Gamma_{22}(N_2 - N_{21}, D_2 - m_{21}) \quad (40a)$$

$$\text{s. t. } 0 \leq N_{21} \leq N_2 - 1. \quad (40b)$$

and problem (39) degrades into

$$\min_{N_{21}} \left(m_{21} + D_1 \Gamma_1(N_1, D_1) \right) \Gamma_{21}(N_{21}, m_{21}) + (D_2 - m_{21}) \Gamma_{22}(N_2 - N_{21}, D_2 - m_{21}) \quad (41a)$$

$$\text{s. t. } 0 \leq N_{21} \leq N_2 - 1. \quad (41b)$$

With convex approximations in Sec. III-A, Problem (40) and (41) can be solved by approach which is more efficient than linear searching N_{21} . With the aids of (33), we also have the convex approximation of SINR function $\Gamma_{21}(N_{21}, m_{21})$. It can be verified that if approximated $\Gamma_{21}(N_{21}, m_{21})$ is convex in N_{21} , then approximated $\Gamma_{22}(N_2 - N_{21}, D_2 - m_{21})$ is also convex in N_{21} , and then the low complexity golden section search method [36] can be modified to find the optimal integer N_{21} . The remaining challenge is that we still cannot have an explicit expression of approximated $\Gamma_{21}(N_{21}, m_{21})$ due to the implicit and complex structure of it. Thanks to the monotonicity with respect to N_k , the bisection search algorithm as in Algorithm 1 can be used to find approximated $\Gamma_{21}(N_{21}, m_{21})$ with given N_{21} . The overall solver with convex approximation is described in Algorithm 3, which consists of 2-D search. The outer search is the linear search of m_{21} and the inner search, from step 4 to 22, is to find the minimum consumed energy for given m_{21} by using the golden section search method, in

Algorithm 3 Proposed convex approximation based algorithm for problem (35)

```

1: Given system parameters  $N_1, N_2, D_1, D_2, \epsilon_1, \epsilon_{21}, \epsilon_{22}$ , and calculate  $f(x_0)$ .
2: for  $m_{21} = \hat{m} : D_2 - \hat{m}$ 
3:   Calculate  $a_{21}, a_{22}, g^{-1}(a_{21}), g^{-1}(a_{22}), f_{21}(g^{-1}(a_{21})), f_{22}(g^{-1}(a_{22}))$ .
4:   Set  $N_{\min} = 0, N_{\max} = N_2$ , and  $A = 0.618$ ;
5:   while  $N_{\max} - N_{\min} \geq \epsilon$  do
6:     Set  $N_\ell = (1 - A)(N_{\max} - N_{\min})$  and  $N_u = A(N_{\max} - N_{\min})$ .

7:   Let  $N_{21} = N_\ell$ 
8:   if  $a_{21} \leq g^{-1}(x_0)$ 
9:     if  $0 \leq N_{21} \leq f_{21}(g^{-1}(a_{21}))$ , Obtain  $\Gamma_{21}(N_{21}, m_{21})$  based on (32);
10:    else Obtain  $\Gamma_{21}(N_{21}, m_{21})$  through bisection search.
11:    end if
12:  else Obtain  $\Gamma_{21}(N_{21}, m_{21})$  through bisection search.
13:  end if
14:  Repeat step 8-13 to calculate  $\Gamma_{22}(N_{22}, m_{22})$  with  $a_{22}$ .
15:  if  $m_{21} \leq D_1$ , Calculate consumed energy  $E_\ell$  based on (40a);
16:  else Calculate  $E_\ell$  based on (41a).
17:  end if
18:  Let  $N_{21} = N_u$ ; Repeat step 7-17 to attain  $E_u$ .
19:  if  $E_\ell \geq E_u$ , Update  $N_{\min} = N_\ell$ ;
20:  else Update  $N_{\max} = N_u$ .
21:  end if
22: end while
23: Set  $N'_\ell = \left\lfloor \frac{N_{\max} + N_{\min}}{2} \right\rfloor$ , and  $N'_u = \left\lceil \frac{N_{\max} + N_{\min}}{2} \right\rceil$ .
24: Calculate  $E'_N(N'_\ell), E'_N(N'_u)$  and let  $E_N^{\text{opt}} = \min \{E'_N(N'_\ell), E'_N(N'_u)\}$ .
25:  $E_N^{\text{opt}} = (E_\ell + E_u)/2$ .
26: if  $E_N^{\text{opt}} \leq E^{\text{opt}}$ , Update  $E^{\text{opt}} = E_N^{\text{opt}}$ .
27: end if
28: end for

```

which step 7-17 is to find the consumed energy with $N_{21} = N_\ell$ where step 8-13 is to find $\Gamma_{21}(N_{21}, m_{21})$ with $N_{21} = N_\ell$.

The computational complexity of Algorithm 3 is shown as follows. Given the latency requirement of receiver 2, D_2 , the outer search of m_{21} needs $\mathcal{O}(D_2 - 2\hat{m})$ rounds to find the optimal m_{21} . In each round, the golden section search will be applied to find the optimal N_{21} with a complexity order of $\mathcal{O}(\log_\phi(\frac{N_2}{\epsilon_0}))$ where $\phi = 1/A$ and A is the golden section search parameter. And, in each golden section search of N_{21} , it contains at most 4 times bisection search to find optimal Γ . Thus the worse case complexity order in each round of golden section search to find N_{21} is given by $\mathcal{O}(4 \log_2(\frac{\max_k \{P_{\max} h_k\}}{\epsilon_0}))$. Summarily, the total complexity of algorithm 3 is bounded by $\mathcal{O}(4(D_2 - 2\hat{m}) \log_2(\frac{N_2}{\epsilon_0}) \log_2(\frac{\max_k \{P_{\max} h_k\}}{\epsilon_0}))$. Compared to algorithm 2, the computation complexity of algorithm 3 is reduced dramatically by transforming the 3-D linear search to a 2-D search approach and further its inner search is conducted by using the efficient golden section search method.

Finally, we present solver for Problem (26). Similar to that in problem (24), we remove the power constraints in problem (26) and solve it with the linear search method. Based on the monotonicity of the energy function in Lemma 1, the optimal m_{21} satisfies $m_{21}^* = m_1$. Thus problem (26) can be solved by 2-D linear search of m_1 and N_{21} . Therefore, for any given

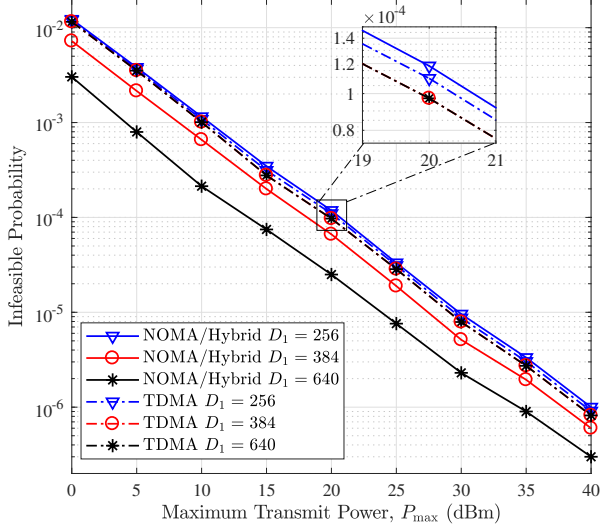


Fig. 7. Infeasible probabilities of proposed transmission schemes with $D_2 = 640$.

m_1 , problem (26) is equivalent to

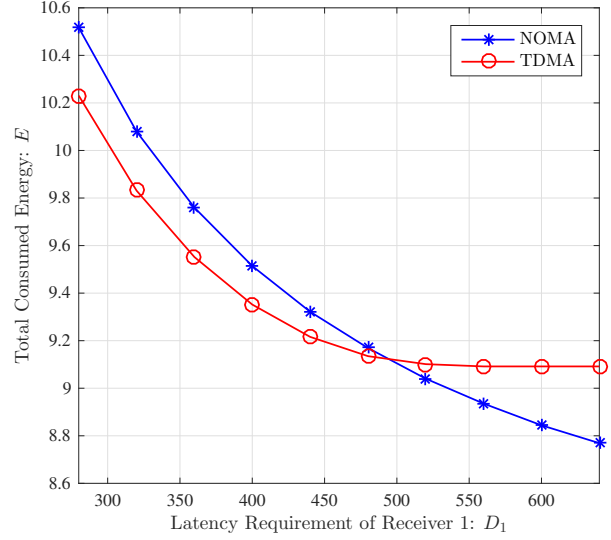
$$\min_{N_{21}} \frac{m_1 \Gamma_1(N_1, m_1) \Gamma_{21}(N_{21}, m_1)}{h_1} + \frac{m_1 \Gamma_{21}(N_{21}, m_1)}{h_2} + \frac{\Gamma_{22}(N_2 - N_{21}, D_2 - m_1)}{h_2} \quad (42a)$$

$$\text{s. t. } 0 \leq N_{21} \leq N_2 - 1. \quad (42b)$$

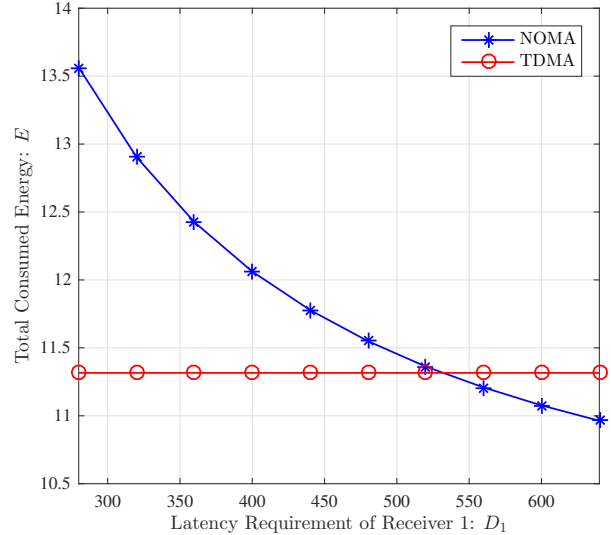
Same as problem (40) and (41), by using the convex approximation of FBC capacity (33), problem (42) can be efficiently solved with the golden section search method.

IV. SIMULATION RESULTS

In this section, simulation results are given to compare the performance of NOMA and hybrid scheme with that of the TDMA under FBC. From the discussions on URLLC in 3GPP [7] [33], we assume that the packets contain equal size of 32 bytes. Also from [7] [33], blocklengths 256, 384 and 640 are adopted for QPSK modulations with channel code rates 1/2, 1/3 and 1/5 respectively. These will be served as benchmarks to choose blocklengths for users D_1 and D_2 in our following simulations. The block error probability of each user is set to be (around) 10^{-6} . For NOMA and the hybrid scheme, we set $\epsilon_1 = \epsilon_2 = 10^{-6}$ and $\epsilon_{21} = \epsilon_{22} = 5 \times 10^{-7}$ such that the error probabilities in (4b) and (23) are both around 10^{-6} . We assume the channel coefficient is composed by the large-scale path loss and the small-scale Rayleigh fading. In particular, the distance-dependent path loss is modeled by $10^{-3}d^{-\alpha}$ where $d = 10$ meter is the Euclidean distance between the transmitter and receiver and $\alpha = 2$ is the path loss exponent; and the variance of the small-scale Rayleigh fading is unity. The energy is obtained by averaging 1000 channel realizations, if without specification. The system bandwidth is 1MHz and the noise power density is set to be $\sigma_1^2 = \sigma_2^2 = -110\text{dBm}$. When $h_1 > h_2$, both problems (7) and (9) are solved and the one that yields the smaller energy is chosen as the consumed



(a) Energy consumption averaged for cases where $h_1 < h_2$.



(b) Energy consumption averaged for cases where $h_1 \geq h_2$.

Fig. 8. Comparisons of consumed energy under NOMA and TDMA with $D_2 = 640$ and $P_{\max} = 40$ dBm.

energy of the NOMA scheme. The energy of TDMA is solved from the successive upper-bound minimization (SUM) method in [17].

As noted in Remark 2, the reliability is determined by the feasibility probability of the optimization problem and the decoding error probability of each user. We set the communication reliability requirement of each user as $1 - 10^{-5}$. With 10^{-6} block error probability, the maximum infeasible probability of the optimization problem is approximately 9×10^{-6} . Now we evaluate the feasibility probability of each scheme and determine the corresponding P_{\max} . Benefit from the feasibility conditions in Remark 1, the feasibility probabilities for NOMA and hybrid schemes are easy to find. Remind that

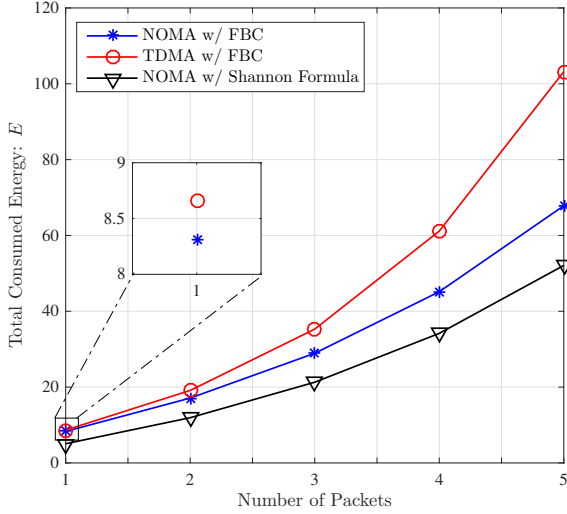
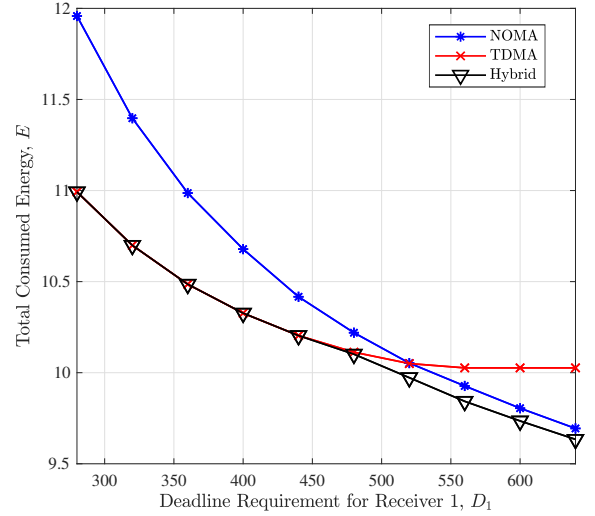


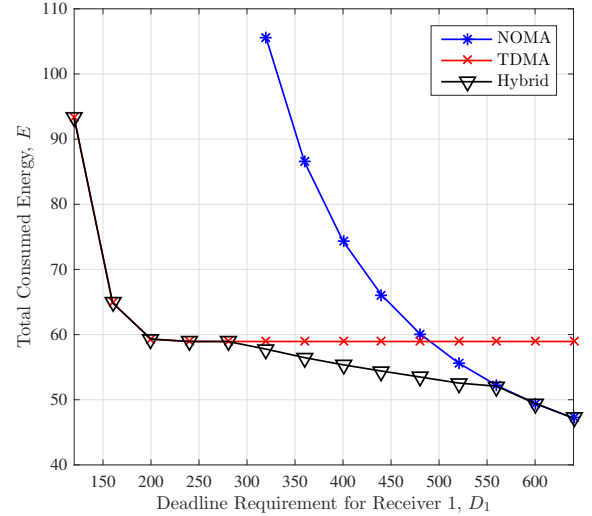
Fig. 9. Energy consumption using FBC and Shannon capacities versus the number of combined packets, with $D_1 = D_2 = 640$, $P_{\max} = 40$ dBm.

NOMA is just a special cases of the hybrid scheme, thus the feasibility of the latter is also checked. The feasibility of TDMA can be checked by checking that of the SUM solver in [17] while the corresponding complexity is much larger than Remark 1. Fig. 7 shows the probabilities when TDMA problem and NOMA problems (5)(7)(9) are infeasible, for different values of latency constraints and maximum available power P_{\max} by performing 10^7 channel realizations. Note that when $P_{\max} \geq 35$ dBm, the infeasible probabilities are all smaller than 4×10^{-6} , thus the overall communication reliability can be satisfied. We thus chose $P_{\max} \geq 35$ dBm in the following simulations. From Fig. 7, one can observe that the infeasible probabilities decrease with the increase of D_1 . It can also be observed that when $D_1 = 256$, the TDMA is a better option; while when $D_1 = 384$ and 640, the NOMA schemes can outperform the TDMA due to that SIC can be efficiently performed at receivers.

Fig. 8 compares the total consumed energy of the NOMA and TDMA schemes with different latency requirements of user 1, in which Fig. 8(a) averages the cases of $h_1 < h_2$ and Fig. 8(b) averages the cases of $h_1 \geq h_2$. As it can be seen in Fig. 8(a), the total consumed energies for both schemes decline with the increase of D_1 . Specifically, for the NOMA scheme, the total consumed energy is strictly decreasing with D_1 . The reason is that, from Section II the optimal blocklength m_1^* of user 1 is D_1 , then a larger D_1 allows a longer m_1^* and thus a smaller power and energy for delivering the packet for user 1. The consumed energy for user 2 is also decreased due to the reduced interference from user 1, and together resulting strictly decreasing energy with increasing D_1 . While for the TDMA scheme, unlike NOMA, the optimal blocklength m_1^* does not always equal to D_1 . When D_1 is small, same as NOMA the optimal $m_1^* = D_1$, and the total consumed energy decreases when D_1 increases. However, when D_1 is large enough, $m_1^* < D_1$ and m_1^* becomes a constant when D_1 increases. As a result, the total consumed energy decreases



(a) Energy consumption with $D_2 = 640$ and $N = 32$, by averaging 1000 channel realizations.



(b) Energy consumption with $D_2 = 640$, $N = 32 \times 3$, and channel realization $h_1 = 300$ and $h_2 = 30$.

Fig. 10. Energy consumption of proposed transmission schemes with $P_{\max} = 40$ dBm and $D_2 = 640$.

first and then keeps unchanged in TDMA. From Fig. 8(b), we can observe that the consumed energy of the TDMA scheme is almost a constant when $D_1 \geq 280$, indicating that the schedule of user 1 is finished before D_1 with high probability due to the good channel condition h_1 . Finally, it is important to note that D_1 approaches D_2 , the NOMA scheme gradually performs better than the TDMA scheme since SIC can effectively reduce the interference as long as it is feasible.

We also compares the energy consumptions predicted by invoking FBC capacity and Shannon capacity in Fig. 9, by fixing latency requirements but varying numbers of transmitted packets. Since it was already pointed out in [17] that the Shannon capacity formula underestimates the energy

for TDMA, we only shows the energy consumption of NOMA by using the Shannon capacity. Again, using Shannon capacity still results in under-estimation of the energy consumption in NOMA. Furthermore, Shannon capacity may not will predict the feasibility of SIC and decoding probabilities may increases. It can be also observed that the performance gain of NOMA compared to TDMA increases with the increase of the number of transmitted packets due to higher spectrum efficiency from non-orthogonal super-position coding. Finally, to investigate the energy consumption of the proposed hybrid scheme, in Fig. 10(a), it is compared with those from pure NOMA and TDMA when the packet size is 32 bytes. One can observe that the proposed hybrid transmission scheme possesses the advantages of both the TDMA and NOMA scheme. Moreover, the hybrid scheme can be even more promising when the packet size is larger than 32 bytes. For example, in Fig. 10(b), when the combined packet size is $32 \times 3 = 96$ bytes, the hybrid scheme can be “strictly” better than both NOMA and TDMA schemes even when D_1 is only half D_2 , that is, $D_1 = 320$. The simulations for Fig 10(b) are performed under $P_{\max} = 40\text{dBm}$, where the infeasible probability is smaller than 7×10^{-6} when $D_1 = 256$.

V. CONCLUSIONS

In this paper, we have considered the energy-efficient transmission design problems subject to heterogeneous and strict latency and reliability constraints at receivers. The FBC has been adopted to explicitly describe the trade-off between latency and reliability. We first investigated the NOMA scheme. However, due to the heterogeneous latency requirements, traditional SIC scheme may not be valid. To cope with this, novel interference mitigation schemes have been proposed. Then by well utilizing the structure of the formulated nonconvex problems in NOMA schemes, optimal transmission powers and code block lengths have been derived and the feasibility of the problem is easy to check. We have found that, due to the heterogeneous latency, the NOMA scheme cannot achieve its best energy efficiency as the traditional ones. In view of this, we have presented a hybrid scheme which can include the TDMA and NOMA as special cases. While the problem is difficult to solve, by approximating the FBC capacity formula, we have proposed the suboptimal but computationally efficient algorithm. The simulation results have shown that the hybrid scheme can possess the advantages of both NOMA and TDMA.

APPENDIX A PROOF OF LEMMA 1

For the simplicity of notations, we remove the subindex of all variables and let x denote the SINR. Based on (5b), we define

$$F(m, x) \triangleq m \ln(x+1) - \sqrt{m} \frac{\sqrt{x(x+2)}}{(x+1)} Q^{-1}(\epsilon) - N \ln 2 = 0, \quad (43)$$

and the partial derivatives of $F(m, x)$ with m and x can be described as

$$F'_m = \ln(x+1) - \frac{Q}{2\sqrt{m}} \frac{\sqrt{x(x+2)}}{x+1}, \quad (44a)$$

$$F'_x = \frac{m}{x+1} - \frac{Q\sqrt{m}}{(x+1)^2 \sqrt{x(x+2)}}. \quad (44b)$$

As is shown in [17], $F'_m > 0$ and $F'_x > 0$ always hold with $m > 0$ and $x > 0$ respectively. The monotonicity of $E(m) = m\Gamma(m)$, where $\Gamma(m) = x$, can be verified by checking the sign of its first derivative. From the implicit function theorem [32]

$$\frac{dE}{dm} = \frac{dmx}{dm} = x + m \frac{dx}{dm} = x - m \frac{F'_m}{F'_x} \triangleq xF'_x - mF'_m, \quad (45)$$

where $A \triangleq B$ denotes that A and B have the same sign. The sign of $\frac{dE}{dm}$ is checked in (46). Note that the right-hand side of (43) is a quadratic equation of \sqrt{m} , and by letting $Q = Q^{-1}(\epsilon)$ and $c = \sqrt{x(x+2)}Q^2 + 4(x+1)^2 \ln(x+1)N \ln 2$, the positive root \sqrt{m} given x in (46c) is

$$\sqrt{m} = \frac{\sqrt{x(x+2)}Q + c}{2(x+1) \ln(x+1)} \quad (47)$$

and it results in (46d); also (46c) and (46f) hold due to $\sqrt{m} > 0$ and $2\sqrt{x(x+2)}(x+1)^2 \ln(x+1) > 0$ for $x > 0$ respectively; (46i) holds because of $x - (x+1) \ln(x+1) < 0$ with $x > 0$ and the fact that $2\sqrt{a+b} \geq \sqrt{2}(\sqrt{a} + \sqrt{b})$ for $a, b > 0$; (46j) holds owing to $\ln(x+1) \geq \frac{2x}{x+2}$ for $x > 0$. In addition, (46m) holds since $x^3(x+2) > 0$ for $x > 0$.

To prove that $E(m)$ is a monotonically decreasing function, we need $f_1(Q, N) < 0$ and $f_2(Q, N) < 0$ in (46), indicating

$$\frac{Q}{\sqrt{N}} \leq \frac{2\sqrt{\ln 2}}{4 - \sqrt{2}} \quad (48)$$

Note that both $f_1(Q, N)$ and $f_2(Q, N)$ increase with Q and decrease with N , and $Q = Q^{-1}(\epsilon)$ is a monotonically decreasing function with ϵ . Therefore, for the pair (ϵ, N) satisfying (48), if we increase ϵ and N , the monotonicity of $E(m)$ also holds. This completes the proof. ■

APPENDIX B PROOF OF PROPOSITION 1

Due to $f(x) \geq 0$, it needs

$$a \leq \frac{(x+1) \ln(x+1)}{\sqrt{x(x+2)}} \triangleq g(x) \quad (49)$$

To verify the monotonicity and convexity of $f(x)$, we give its first and second-order derivatives as follows

$$f'(x) = \frac{1}{x+1} - \frac{a}{(x+1)^2 \sqrt{x(x+2)}}, \quad (50a)$$

$$f''(x) = \frac{-1}{(x+1)^2} + \frac{a(2(x(x+2)) + (x+1)^2)}{(x+1)^3 (x(x+2))^{\frac{3}{2}}} \quad (50b)$$

To guarantee $f(x)$ a monotonically increasing function, we require $f'(x) \geq 0$. Thus it needs

$$a \leq (x+1) \sqrt{x(x+2)} \triangleq g_1(x) \quad (51)$$

$$\frac{dE}{dm} \triangleq xF'_x - mF'_m = \frac{mx}{x+1} - \frac{Q\sqrt{m}x}{(x+1)^2\sqrt{x(x+2)}} - m\ln(x+1) + \frac{Q\sqrt{m}}{2} \frac{\sqrt{x(x+2)}}{x+1} \quad (46a)$$

$$= \left(\frac{x}{x+1} - \ln(x+1) \right) m + \frac{(x+1)(x(x+2)) - 2x}{2(x+1)^2\sqrt{x(x+2)}} Q\sqrt{m} \quad (46b)$$

$$\triangleq \left(\frac{x}{x+1} - \ln(x+1) \right) \sqrt{m} + \frac{x^3 + 3x^2}{2(x+1)^2\sqrt{x(x+2)}} Q \quad (46c)$$

$$= \left(\frac{x}{x+1} - \ln(x+1) \right) \frac{\sqrt{x(x+2)}Q + c}{2(x+1)\ln(x+1)} + \frac{x^3 + 3x^2}{2(x+1)^2\sqrt{x(x+2)}} Q \quad (46d)$$

$$= \frac{x\sqrt{x(x+2)}Q + cx}{2(x+1)^2\ln(x+1)} - \frac{\ln(x+1)\sqrt{x(x+2)}Q + c\ln(x+1)}{2(x+1)\ln(x+1)} + \frac{x^3 + 3x^2}{2(x+1)^2\sqrt{x(x+2)}} Q \quad (46e)$$

$$\triangleq x^2(x+2)Q + cx\sqrt{x(x+2)} - x(x+1)(x+2)\ln(x+1)Q - c(x+1)\sqrt{x(x+2)}\ln(x+1) + (x^3 + 3x^2)\ln(x+1)Q \quad (46f)$$

$$= (x^2(x+2) - (x^3 + 3x^2 + 2x)\ln(x+1) + (x^3 + 3x^2)\ln(x+1))Q + (x - (x+1)\ln(x+1))\sqrt{x(x+2)}c \quad (46g)$$

$$= (x^2(x+2) - 2x\ln(x+1))Q + (x - (x+1)\ln(x+1))\sqrt{x(x+2)}\sqrt{x(x+2)}Q^2 + 4N(x+1)^2\ln(x+1)\ln 2 \quad (46h)$$

$$\leq (x^2(x+2) - 2x\ln(x+1))Q + \frac{\sqrt{2}}{2} (x - (x+1)\ln(x+1))\sqrt{x(x+2)} \left(\sqrt{x(x+2)}Q^2 + \sqrt{4N(x+1)^2\ln(x+1)\ln 2} \right) \quad (46i)$$

$$\leq \left(x^2(x+2) - 2x\frac{2x}{x+2} \right) Q + \frac{\sqrt{2}}{2} \left(x - (x+1)\frac{2x}{x+2} \right) x(x+2)Q + \sqrt{2} \left(x - (x+1)\frac{2x}{x+2} \right) (x+1)\sqrt{x(x+2)}\sqrt{\frac{2x}{x+2}N\ln 2} \quad (46j)$$

$$= (x^2(x+2)^2 - 4x^2)(x+2)Q - \frac{\sqrt{2}}{2} x^3(x+2)^2Q - \sqrt{2}x^2(x+1)\sqrt{x(x+2)}\sqrt{2x(x+2)N\ln 2} \quad (46k)$$

$$= x^3(x+4)(x+2)Q - \frac{\sqrt{2}}{2} x^3(x+2)^2Q - 2x^3(x+1)(x+2)\sqrt{N\ln 2} \quad (46l)$$

$$\triangleq 2(x+4)Q - \sqrt{2}(x+2)Q - 4(x+1)\sqrt{N\ln 2} \quad (46m)$$

$$= \underbrace{(2Q - \sqrt{2}Q - 4\sqrt{N\ln 2})x}_{f_1(Q,N)} + \underbrace{8Q - 2\sqrt{2}Q - 4\sqrt{N\ln 2}}_{f_2(Q,N)}. \quad (46n)$$

It can be easily proved that $g_1(x) \geq g(x)$ for $x \geq 0$, which implies that if the finite blocklength capacity formula holds then $f(x)$ is a monotonically increasing function. Further, to guarantee $f(x)$ a concave function, we require $f''(x) \leq 0$ and have

$$f''(x) = \frac{-1}{(x+1)^2} + \frac{a(2(x(x+2)) + (x+1)^2)}{(x+1)^3(x(x+2))^{\frac{3}{2}}} \quad (52a)$$

$$= \frac{a(3x^2 + 6x + 1) - (x+1)(x(x+2))^{\frac{3}{2}}}{(x+1)^3(x(x+2))^{\frac{3}{2}}} \quad (52b)$$

$$\triangleq a(3x^2 + 6x + 1) - (x+1)(x(x+2))^{\frac{3}{2}} \leq 0 \quad (52c)$$

or equivalently

$$a \leq \frac{(x+1)(x(x+2))^{\frac{3}{2}}}{3x^2 + 6x + 1} \triangleq g_2(x) \quad (53)$$

On the contrary, when $a \geq g_2(x)$, $f(x)$ is convex.

With some algebraic manipulations, we can find that $g(x)$ and $g_2(x)$ are monotonically increasing functions, and $g_2(x) \leq g(x)$ for $0 \leq x \leq x_0$; $g_2(x) > g(x)$ for $x > x_0$ where $x_0 = 0.6904$ is the positive solution of equation $g_2(x) = g(x)$. Therefore, for given parameter a and defining $\beta \triangleq g(x_0) = g_2(x_0)$, if $a > \beta$, $f(x)$ is concave for $x \geq g^{-1}(a)$; if $a \leq \beta$, $f(x)$ is convex for $g^{-1}(a) \leq x \leq g_2^{-1}(a)$ and concave for $x > g_2^{-1}(a)$. This completes the proof. ■

REFERENCES

- [1] Y. Xu, C. Shen, T.-H. Chang, S.-C. Lin, Y. Zhao, and G. Zhu, "Energy-efficient non-orthogonal transmission under reliability and blocklength constraints," in *Proc. IEEE GlobeCom Workshop on Ultra-Reliable and Low-Latency Communications.*, Dec. 2017. Singapore.
- [2] 3GPP, *Study on Scenarios and Requirements for Next Generation Access Technologies.* Technical Report 38.913, Release 14, Otc. 2016.
- [3] G. Durisi, T. Koch, and P. Popovski, "Toward massive, ultrareliable, and low-latency wireless communication with short packets," *Proc. IEEE*, vol. 104, no. 9, pp. 1711–1726, Sep. 2016.
- [4] P. Popovski, "Ultra-reliable communication in 5G wireless systems," in *1st Int. Conf. 5G for Ubiquitous Connectivity*, Nov. 2014, pp. 146–151.
- [5] P. Popovski, J. J. Nielsen, C. Stefanovic, E. d. Carvalho, E. Strom, K. F. Trillingsgaard, A. S. Bana, D. M. Kim, R. Kotaba, J. Park, and R. B. Sorensen, "Wireless access for ultra-reliable low-latency communication: Principles and building blocks," *IEEE Network*, vol. 32, no. 2, pp. 16–23, Mar. 2018.
- [6] C. She, C. Yang, and T. Q. S. Quek, "Radio resource management for ultra-reliable and low-latency communications," *IEEE Commun. Mag.*, vol. 55, no. 6, pp. 72–78, Jun. 2017.
- [7] 3GPP, *Summary of email discussion on the link level evaluation for LTE URLLC.* TSG RAN WG1 Meeting #92, R1-1801385, Mar. 2018. Available: http://www.3gpp.org/ftp/Meetings_3GPP_SYNC/RAN1/Docs/.
- [8] J. Andrews, S. Buzzi, C. Wan, S. Hanly, A. Lozano, A. Soong, and J. Zhang, "What will 5G be?" *IEEE J. Sel. Areas Commun.*, vol. 32, no. 6, pp. 1065–1082, Jun. 2014.
- [9] X. Wang and Z. Q. Li, "Energy-efficient transmissions of bursty data packets with strict deadlines over time-varying wireless channels," *IEEE Trans. Wireless Commun.*, vol. 12, no. 5, pp. 2533–2543, May 2013.
- [10] W. S. Chen, U. Mitra, and M. J. Neely, "Energy-efficient scheduling with individual packet delay constraints over a fading channel," *Wireless Netw.*, vol. 15, no. 5, pp. 601–618, Jul. 2009.

- [11] C. E. Shannon, "A mathematical theory of communication," *The Bell Sys. Tech. Journal*, vol. 27, no. 3, pp. 379–423, Jul. 1948.
- [12] T. Cover and J. Thomas, *Elements of Information Theory*. New York: Wiley, 1991.
- [13] Y. Polyanskiy, H. V. Poor, and S. Verdú, "Channel coding rate in the finite blocklength regime," *IEEE Trans. Inf. Theory*, vol. 56, no. 5, pp. 2307–2359, May 2010.
- [14] Y. Polyanskiy and S. Verdú, "Scalar coherent fading channel: Dispersion analysis," in *Proc. IEEE ISIT*, Aug. 2011. St. Petersburg, Russia, pp. 2959–2963.
- [15] W. Yang, G. Durisi, T. Koch, and Y. Polyanskiy, "Quasi-static multiple-antenna fading channels at finite blocklength," *IEEE Trans. Inf. Theory*, vol. 60, no. 7, pp. 4232–4265, Jul. 2014.
- [16] B. Li, H. Shen, and D. Tse, "An adaptive successive cancellation list decoder for polar codes with cyclic redundancy check," *IEEE Commun. Lett.*, vol. 16, no. 12, pp. 2044–2047, Dec. 2012.
- [17] S. Xu, T.-H. Chang, S.-C. Lin, C. Shen, and G. Zhu, "Energy-efficient packet scheduling with finite blocklength codes: Convexity analysis and efficient algorithms," *IEEE Trans. Wireless Commun.*, vol. 15, no. 8, pp. 5527–5540, Aug. 2016.
- [18] G. Ozcan and M. Gursoy, "Throughput of cognitive radio systems with finite blocklength codes," *IEEE J. Sel. Areas in Comm.*, vol. 31, no. 11, pp. 2541–2554, Nov. 2013.
- [19] M. C. Gursoy, "Throughput analysis of buffer-constrained wireless systems in the finite blocklength regime," *EURASIP J. Wirel. Comm.*, vol. 2013, no. 1, pp. 1–13, 2013.
- [20] B. Makki, T. Svensson, and M. Zorzi, "Finite block-length analysis of spectrum sharing networks: Interference-constrained scenario," *IEEE Wireless Commun. Lett.*, vol. 4, no. 4, pp. 433–436, 2015.
- [21] —, "Wireless energy and information transmission using feedback: Infinite and finite block-length analysis," *IEEE Trans. Commun.*, vol. 64, pp. 5304–5318, Dec. 2016.
- [22] Y. Hu, A. Schmeink, and J. Gross, "Blocklength-limited performance of relaying under quasi-static Rayleigh channels," *IEEE Trans. Wireless Commun.*, vol. 15, no. 7, pp. 4548–4558, Jul. 2016.
- [23] Y. Hu, J. Gross, and A. Schmeink, "On the capacity of relaying with finite blocklength," *IEEE Trans. Veh. Techn.*, vol. 65, no. 3, pp. 1790–1794, Mar. 2016.
- [24] C. She, C. Yang, and T. Q. S. Quek, "Cross-layer optimization for ultra-reliable and low-latency radio access networks," *IEEE Trans. Wireless Commun.*, vol. 17, no. 1, pp. 127–141, Jan. 2018.
- [25] Z. Ding, Y. Liu, J. Choi, Q. Sun, M. Elkashlan, C. L. I, and H. V. Poor, "Application of non-orthogonal multiple access in LTE and 5G networks," *IEEE Commun. Mag.*, vol. 55, no. 2, pp. 185–191, Feb. 2017.
- [26] Y. Xu, C. Shen, Z. Ding, X. Sun, S. Yan, G. Zhu, and Z. Zhong, "Joint beamforming and power splitting control in downlink cooperative SWIPT NOMA systems," *IEEE Trans. Signal Process.*, vol. 15, no. 18, pp. 4874–4886, Sep. 2017.
- [27] 3GPP, *Study on Downlink Multiuser Superposition Transmission*. Technical Report 36.859, Dec. 2015.
- [28] Y. Hu, M. C. Gursoy, and A. Schmeink, "Efficient transmission schemes for low-latency networks: NOMA vs. relaying," in *Proc. 2017 PIMRC*, Oct. 2017.
- [29] Y. Yu, H. Chen, Y. Li, Z. Ding, and B. Vucetic, "On the performance of non-orthogonal multiple access in short-packet communications," *IEEE Commun. Lett.*, vol. 22, no. 3, pp. 590–593, Mar. 2017.
- [30] X. Sun, S. Yan, N. Yang, Z. Ding, C. Shen, and Z. Zhong, "Short-packet communications in non-orthogonal multiple access systems," available: <https://arxiv.org/pdf/1704.06420>.
- [31] K. F. Trillingsgaard and P. Popovski, "Downlink transmission of short packets: Framing and control information revisited," *IEEE Trans. Commun.*, vol. 65, pp. 2048–2061, May 2017.
- [32] S. G. Krantz and H. R. Parks, *The Implicit Function Theorem: History, Theory, and Applications*. Boston, MA: Birkhäuser, 2002.
- [33] 3GPP, *Discussion on PDSCH related techniques for URLLC*. TSG RAN WG1 Meeting #92, R1-1801776, Mar. 2018. Available: http://www.3gpp.org/ftp/Meetings_3GPP_SYNC/RAN1/Docs/.
- [34] S. Boyd and L. Vandenberghe, *Convex Optimization*. Cambridge Univ. Press, 2009.
- [35] M. Mila, "Convexity of the inverse function," *Teach. Math.*, vol. 11, no. 1, pp. 21–24, 2008.
- [36] W. H. Press, S. A. Teukolsky, and W. T. Vetterling, *Section 10.2. Golden Section Search in One Dimension, Numerical Recipes: The Art of Scientific Computing*. New York: Cambridge Univ. Press, 2007.